Structural and spectroscopic studies of azide complexes of horse heart myoglobin and the His-64 → Thr variant

Robert MAURUS, Ralf BOGUMIL[1], Nham T. NGUYEN, A. Grant MAUK[2] and Gary BRAYER

Department of Biochemistry and Molecular Biology and the Protein Engineering Network of Centres of Excellence, University of British Columbia, Vancouver, British Columbia V6T 1Z3, Canada

The high-resolution X-ray crystallographic structures of horse heart azidometmyoglobin complexes of the wild-type protein and the His-64 → Thr variant have been determined to 2.0 and 1.8 Å respectively. Azide binds to wild-type metmyoglobin in a bent configuration with an Fe–N-1–N-3 angle of 119° and is oriented into the distal crevice in the direction of Ile-107. The proximity of the His-64 NE2 atom to the N-1 atom of the bound azide indicates stabilization of the ligand by the His-64 side chain through hydrogen bonding. In addition, structural characterization of wild-type horse heart azidometmyoglobin establishes that the only structural change induced by ligand binding is a small movement of the Leu-29 side chain away from the azide ligand. EPR and Fourier transform infrared spectroscopy were used to characterize the myoglobin azide complexes further. EPR spectroscopy revealed that, in contrast with wild-type azidometmyoglobin, two slightly different low-spin species are formed by azide bound to the His-64 → Thr variant both in solution and in a polycrystalline sample. One of these low-spin species has a greater relative intensity, with $\boldsymbol{g}$ values very similar to those of the azide complex of the wild-type protein. These EPR results together with structural information on this variant indicate the presence of two distinct conformations of bound azide, with one form predominating. The major conformation is comparable to that formed by wild-type myoglobin in which azide is oriented into the distal crevice. In the minor conformation the azide is oriented towards the exterior of the protein.

INTRODUCTION

Recent efforts have contributed to a detailed understanding of ligand binding to haemoglobin and myoglobin and of the role of the surrounding protein structure in this process [1–8]. Particular attention has been directed at the role of the proximal His-93 residue and the distal His-64 residue, which can stabilize binding of exogenous ligands through hydrogen-bonding interactions. Considerable insight has been gained by the characterization of the ligand-binding properties of myoglobin variants in which His-64 has been replaced (reviewed in [9]). From this work it is now known that the replacement of His-64 with non-polar residues (valine, leucine, phenylalanine and isoleucine) leads to pentaco-ordinated ferric haem proteins lacking a distally co-ordinated water molecule [10–16]. The loss of this bound water molecule is primarily attributable to two factors: (1) the additional hydrophobicity of the non-polar residues introduced at position 64, and (2) the disruption of the stabilizing hydrogen bond between the distal histidine residue and the co-ordinated water molecule.

In the ferric state, myoglobin can bind a variety of anions such as N_3^-, CN^-, SCN^- and F^-. The N_3^- anion has been used widely to prepare stable low-spin iron Fe(III) haem protein derivatives. This charged group prefers a bent conformation when co-ordinated to the haem iron in both myoglobin [17,18] and haemoglobin [19,20]. The structural factors governing N_3^- and CN^- binding have been examined more recently [18,21], and it has been suggested that steric hindrance by His-64 is a key factor in the regulation of the association rate of azide [21]. For example, greater association rate constants are observed when His-64 is replaced by smaller residues such as glycine, alanine, and threonine. However, the affinity of wild-type myoglobin for N_3^- is greater than that exhibited by most position 64 variants owing to the greater rate of N_3^- dissociation from the variants. The lower rate of N_3^- dissociation from wild-type myoglobin can be explained by the stabilizing effect of hydrogen-bonding interactions between His-64 and co-ordinated N_3^- [21,22].

We previously analysed the interaction of N_3^- with several horse heart myoglobin variants, including His-64 variants, with Fourier transform infrared (FTIR) spectroscopy [22]. This work demonstrated that the electrostatic potential surrounding the bound ligand is one important factor governing the ν_{max} of the asymmetric N_3^- stretch, because the introduction of positively or negatively charged surface residues shifted the ν_{max} in opposite directions compared with wild-type myoglobin without a significant change in bandwidth. More drastic changes were observed in the FTIR spectra of His-64 variants, which could in part be explained by the disruption of the proposed hydrogen bond between His-64 and the bound N_3^- ligand.

To further our understanding of the interaction of N_3^- with metmyoglobin, we have now determined the high resolution structures of N_3^- complexes formed by wild-type horse heart myoglobin and the His-64 → Thr variant. These structural data allow a more detailed analysis of the spectroscopic data and help to explain spectroscopic differences between wild-type and His-64 → Thr N_3^- complexes. To assist this analysis, additional spectroscopic measurements of the N_3^- complexes are presented both for samples in solution and those in the polycrystalline state.

EXPERIMENTAL

Mutagenesis and protein purification

Recombinant wild-type horse heart myoglobin and the His-64 → Thr variant were prepared as described previously [22–24].

Abbreviations used: FTIR, Fourier transform, infrared; MbN_3^-, azidometmyoglobin; Wat, water.

[1] Present address: Biochemisches Institut der Universität Zürich, Winterhurestrasse 190, CH-8057 Zürich, Switzerland.

[2] To whom correspondence should be addressed.

FTIR spectroscopy

Spectra were recorded at 2 cm^{-1} resolution with a Perkin-Elmer System 2000 FTIR spectrometer equipped with a liquid-nitrogen-cooled mercury cadmium telluride detector. N_3^- complexes were formed by mixing concentrated myoglobin solutions (approx. 4 mM) in 20 mM Tris buffer (pH 8.0) or phosphate buffer (pH 7.5) with small amounts of 40 mM NaN_3 solution dissolved in the same buffer. In each case a slight excess of myoglobin was used to minimize bands attributable to free N_3^-. An average of 400 scans was obtained, and data collection and curve fitting were performed by the method of Bogumil et al. [22].

EPR spectroscopy

Samples of metmyoglobin (1–1.5 mM) in 20 mM Tris/HCl buffer, pH 8.0, were mixed with concentrated NaN_3 solution in the same buffer. For analysis of a polycrystalline sample, several small crystals of the His-64 → Thr variant were suspended in 65 %-satd. $(NH_4)_2SO_4$ in 20 mM Tris/HCl, pH 8.0. EPR spectra were obtained at X-band frequencies (approx. 9.5 GHz) with a Bruker Model ESP 300E spectrometer equipped with an Oxford Instruments liquid-helium cryostat and an Oxford Instruments ITC4 temperature controller. The experimental conditions used were 10 K, 0.63 mW microwave power, 9.45 GHz microwave frequency, 100 kHz modulation frequency and 1 mT modulation amplitude.

Structure determination

Crystals of the azidometmyoglobin (MbN_3^-) complexes of recombinant wild-type metmyoglobin and the His-64 → Thr variant were grown at room temperature (25 °C) by the hanging-drop vapour diffusion method. For wild-type myoglobin, a 5 μl hanging droplet (pH 7.5) containing 15 mg/ml protein, 60 %-satd. $(NH_4)_2SO_4$, 20 mM Tris/HCl, 5 mM NaN_3 and 1 mM EDTA was suspended over a well containing 1.0 ml (pH 7.5) of 65 %-satd. $(NH_4)_2SO_4$, 20 mM Tris/HCl and 1 mM EDTA. For the His-64 → Thr variant, the 5 μl hanging droplet (pH 8.4) contained 15 mg/ml protein, 65 %-satd. $(NH_4)_2SO_4$, 20 mM Tris/HCl, 25 mM NaN_3 and 1 mM EDTA and was suspended over a well (pH 8.4) containing 1.0 ml of 70 %-satd. $(NH_4)_2SO_4$, 20 mM Tris/HCl and 1 mM EDTA. For both proteins, crystals grew to a maximum size of 0.2 mm × 0.1 mm × 0.05 mm in approx. 10 weeks and were isomorphous with those grown for wild-type [25] and recombinant wild-type [26] horse heart metmyoglobins. Space group and unit cell parameters for MbN_3^- crystals are shown in Table 1.

Diffraction data sets for the N_3^- forms of the recombinant myoglobin and the His-64 → Thr variant were collected with a Rigaku R-Axis II imaging plate area detector system to 2.0 and 1.8 Å resolution respectively. This area detector used CuK_α radiation generated from a rotating anode fitted with a monochromator and operated at 90 mA and 59 kV. For each data collection frame, the crystal was oscillated through an angle of 1.5° and exposed to the X-ray beam for 30–45 min. The crystal-to-detector distance was 78 mm. X-ray intensity data were processed to structure factors with the R-AXIS II data processing software [27,28], which is based on techniques described by Rossman et al. [29].

Given the isomorphous unit cells involved, a restrained-parameter least-squares approach [30] was employed to refine the recombinant wild-type MbN_3^-, with the structure of recombinant wild-type horse heart metmyoglobin [26] as the starting model. For the variant MbN_3^-, the structure of the His-64 → Thr variant [16] was used as the starting model. For both proteins, inspection of initial F_0-F_c difference electron density maps showed the presence of the N_3^- ligands unambiguously. Thus initial refinement of both structures started with the inclusion of an N_3^- ligand modelled as a linear triatomic molecule [31]. Also included in the initial refinement models were well-defined water molecules ($B < 35$ Å^2) and a sulphate ion found in the original recombinant wild-type myoglobin structure. Care was taken to exclude water molecules within 6 Å of the bound N_3^- ligand from the starting refinement model.

During the course of refinements, omit, F_0-F_c and $2F_0-F_c$ difference electron density maps covering the entire polypeptide chain of each protein were examined at two different times. Doing so permitted the manual adjustment of a number of surface main- and side-chain conformations as well as that of the N_3^- ligand. For both structures, the C-terminal residues 152–153 were disordered in electron density maps and were modelled by finding a geometrically reasonable configuration that maximized the use of the electron density present. Additional water molecules were found by searching F_0-F_c difference electron density maps. These water molecules were restricted to those having reasonable hydrogen bonds to protein atoms, and thermal factors that refined to less than 60 Å^2. Refinement was concluded when positional shifts became small (overall root-mean-square shifts < 0.03 Å), indicating that convergence had been reached. Final refinement parameters are shown in Table 1 along with statistics related to the stereochemistry of the final refinement models.

Atomic coordinate errors for both MbN_3^- structures were estimated by two methods. Inspection of a Luzzati [32] plot suggests overall root-mean-square coordinate errors of 0.18 and 0.20 Å for the wild-type and variant MbN_3^- proteins respectively. The corresponding estimates obtained by the method of Cruickshank [33–35] are 0.12 and 0.16 Å.

Table 1 Data collection and refinement parameters for the structures of wild-type and His-64 → Thr MbN_3^-

Parameters	Wild-type	His-64 → Thr
(I) Data collection		
Space group	$P2_1$	$P2_1$
Cell dimensions (Å)		
a	64.3	64.0
b	28.9	28.8
c	35.9	35.8
β (degrees)	107.2	107.0
No. of accepted measurements	14776	19842
No. of unique reflections	5531	8046
Merging R-factor (%)*	10.2	9.1
(II) Refinement		
No. of reflections used	5260	7631
Resolution range (Å)	6.0–2.0	6.0–1.8
No. of protein atoms	1242	1239
No. of solvent molecules	59	51
Average thermal factors (Å^2)		
Protein atoms	21.0	17.4
Solvent atoms	29.8	26.3
Final refinement R-factor (%)†	17.3	17.8

* $R_{merge} = \left(\sum_{hkl}\sum_{i=0}^{n} |I_{i_{hkl}} - \bar{I}_{hkl}|\right) \Big/ \left(\sum_{hkl}\sum_{i=0}^{n} I_{i_{hkl}}\right)$.

† $R\text{-factor} = \sum_{hkl} |F_0 - F_c| / \sum_{hkl} |F_0|$.

RESULTS

EPR and FTIR spectroscopy

Initial inspection of difference electron density maps in the distal haem region of the N_3^- complex of the His-64 → Thr variant suggested that N_3^- binds to this protein in more than one orientation. To investigate this unexpected feature further, spectroscopic techniques were applied. The EPR spectra of the N_3^- complexes of the wild-type and variant myoglobins are shown in Figure 1. These spectra are characteristic of ferric low-spin haem proteins. The N_3^- complex of the wild-type protein exhibits one low-spin species (Figure 1, trace A; *g* values 2.80, 2.21 and 1.72) that is similar to spectra recorded previously for the N_3^- complex of horse heart and sperm whale myoglobin [22,36]. In contrast, two slightly different low-spin species were observed in the spectra of the His-64 → Thr N_3^- adduct in solution (Figure 1, trace B) and in a polycrystalline sample (Figure, trace C). Both low-spin species exhibit *g* values in the range expected for MbN_3^- complexes and are consistent with the binding of N_3^- in two orientations. One of these low-spin species has a greater relative intensity (Figure 1, trace B) and *g* values (2.78, 2.22 and 1.73) that correspond to those of the N_3^- complex formed by wild-type myoglobin.

To determine whether differences in the relative intensities of the two N_3^- complexes of the variant might be caused by $(NH_4)_2SO_4$ present in the crystalline sample, successive amounts of this salt were added to the sample in solution. The resulting EPR spectra were slightly broadened, but the relative amounts of the two species were comparable to the sample with no $(NH_4)_2SO_4$ present, therefore ruling out the possible influence of $(NH_4)_2SO_4$ in setting the relative peak intensity. Addition of the glassing agent glycerol to the sample in solution resulted in only a small decrease in the less intense species (results not shown).

A buffer-dependence of the EPR spectra of some five-co-ordinated His-64 variants has been reported [11,16]. Our results also show a dependence of the EPR spectra of the N_3^- complex formed by the His-64 → Thr variant on the buffer used. Thus whereas the spectra in 50 mM Hepes (pH 7; results not shown) and spectra obtained for samples in Tris buffer (Figure 1, trace B) exhibit two low-spin forms, spectra obtained for samples in phosphate buffer (pH 7) exhibit just one form [22]. As with the observations of Ikeda-Saito et al. [11], the origin of this buffer-dependence is unknown.

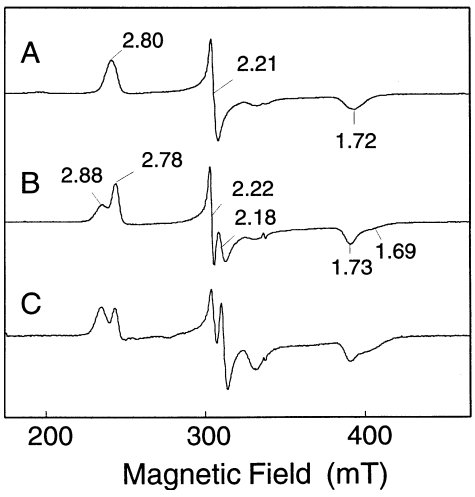

Figure 1 X-band EPR spectra of wild-type and variant MbN_3^- complexes (10 K, 20 mM Tris/HCl buffer, pH 8.0)

Trace A, wild-type myoglobin frozen solution; trace B, His-64 → Thr variant frozen solution; trace C, polycrystalline H-64 → Thr variant in 65%-satd. $(NH_4)_2SO_4$.

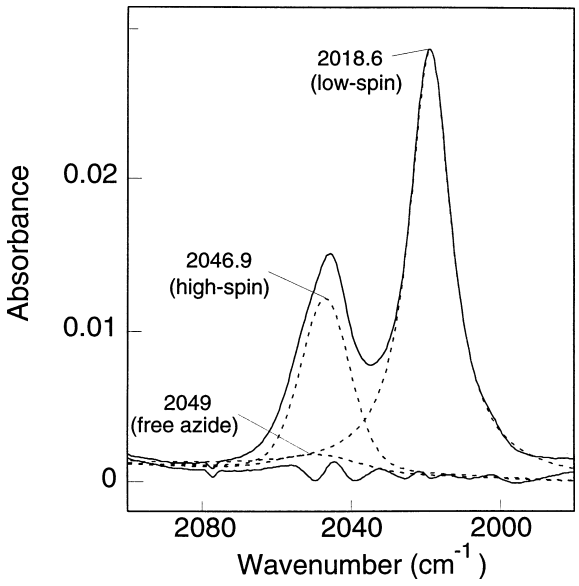

Figure 2 Infrared spectrum of the His64Thr variant MbN_3^- complex (277 K, 20 mM Tris/HCl buffer, pH 8.0)

Upper solid line, experimental spectrum; broken lines, deconvoluted absorption bands; lower solid line, experimental spectrum minus deconvoluted components.

The FTIR spectra of the N_3^- complexes of several myoglobin variants in phosphate buffer (pH 7) were reported previously [22]. Because the EPR spectrum of the His-64 → Thr N_3^- complex depends on buffer composition, the FTIR spectrum of this derivative was also examined in 20 mM Tris buffer (pH 8.0), the conditions used for crystallization of this complex. The resulting FTIR spectrum in the region of the asymmetric stretching vibration of the azide ion is shown in Figure 2. The two bands at 2018.6 and 2045.9 cm^{-1} can be assigned to the low-spin and high-spin forms of bound N_3^- respectively. For the N_3^- complex of wild-type metmyoglobin, the respective IR bands exhibit significantly narrower line widths and occur at 2023.7 (low-spin) and 2046.1 cm^{-1} (high-spin). The N_3^- complexes of both the wild-type and variant proteins exhibit a temperature-dependent spin equilibrium, with a 70–80% low-spin component at 293 K. With increasing temperature the abundance of the high-spin component increases. Because the low-spin form is more sensitive to changes in the immediate environment, FTIR spectra were obtained at 277 K where this form dominates. Both the ν_{max}(2018.6 cm^{-1}) and the half bandwidth (13.8 cm^{-1}) of the low-spin band of the His-64 → Thr protein are nearly identical with the respective FTIR spectra of samples prepared in phosphate buffer (ν_{max} 2018.6 cm^{-1}; half bandwidth 13.5 cm^{-1}), indicating that the buffer dependence seen in the EPR spectra might result from low temperature and/or freezing effects.

FTIR spectroscopy is a sensitive method for observing the conformational diversity of bound ligands (see, for example, [37,38]). Although curve fitting of the data for the His-64 → Thr MbN_3^- complex is consistent with the presence of only one low-spin band, the line width observed is significantly greater than that of wild-type MbN_3^- (half bandwidth 8.3 cm^{-1}). This difference could result from a greater orientational variability of N_3^- bound to the variant or the presence of more than one conformation of the bound N_3^-.

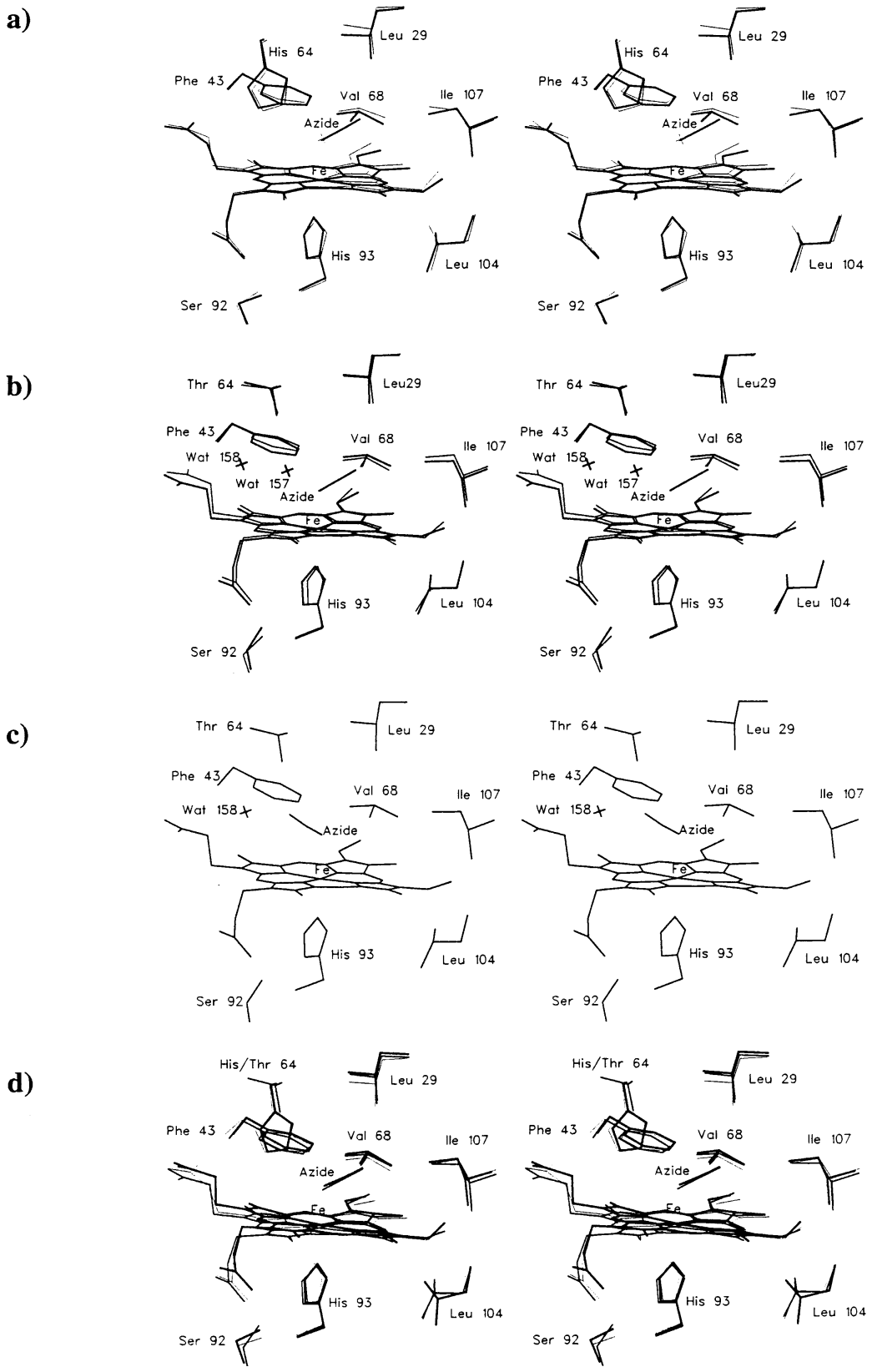

Figure 3 For legend see opposite page

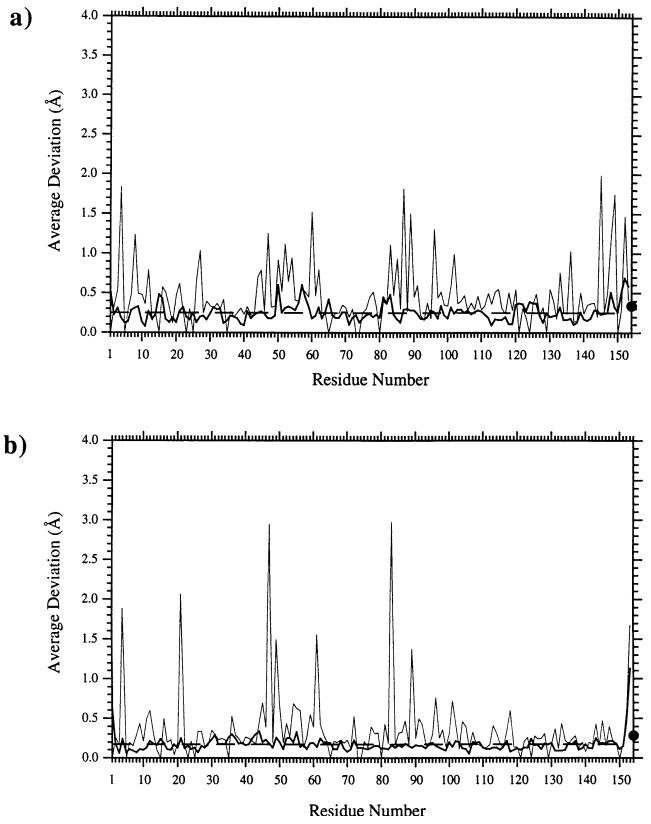

Figure 4 Average positional deviations between the main-chain (thick lines) and side-chain atoms (thin lines) of horse heart metmyoglobins

(**a**) Wild-type aquo- and azidometmyoglobin; (**b**) His-64 → Thr aquo- and azidometmyoglobin. The horizontal broken line on each figure represents the overall deviation between all main-chain atoms. The filled circle at residue 154 represents the average deviation for all 43 haem atoms.

Structure of the wild-type MbN_3^- complex

N_3^- bound to the haem iron of wild-type myoglobin is oriented in the direction of Leu-29 and Ile-107 (Figure 3) and is completely inaccessible to solvent. In this position, the co-ordinated N_3^- is adjacent to the side chain of His-64, and the N-E2 nitrogen atom of this residue is within hydrogen-bonding distance (2.8 Å) of the N-1 nitrogen atom bound to the haem iron. The observed haem iron-to-N_3^- distance is 2.11 Å, and the corresponding bonding angle (Fe–N-1–N-3) is 119°. The N_3^- ligand refined to full occupancy with thermal factors of 22, 23 and 21 Å² for its N-1, N-2 and N-3 atoms respectively. These values are comparable to the average thermal factor of 21 Å² found for all other protein atoms in the structure of recombinant wild-type myoglobin [26].

To facilitate comparison of the wild-type and variant MbN_3^- structures, they were superimposed with a least-squares fit based on all main chain atoms. A plot of the resultant main-chain and side-chain positional differences is presented in Figure 4. These results indicate an overall average deviation of 0.25 Å for all main-chain atoms. The largest displacements occur at the two polypeptide chain termini (residues 1 and 151–153, Δd 0.55 and 0.60 Å respectively), Gly-15 (Δd 0.48 Å), *Lys*-50 (Δd 0.60 Å), *Ala*-57 (Δd 0.60 Å), His-81 to Glu-83 (Δd 0.43 Å) and Gly-148 (Δd 0.51 Å).

The residues in the haem-binding pocket are positioned similarly in the N_3^--bound and N_3^--free structures. The only notable exception is the side chain of Leu-29 (Δd 0.40 Å for side-chain atoms), which is in van der Waals contact with the N_3^- ligand (Figure 3). Notably, however, the position of the haem group shifts on N_3^- binding. If only the positions of haem atoms are superimposed, the overall average positional difference is 0.18 Å. These shifts involve movement of the haem in the direction of Leu-104 (Figure 3). The most notable deviations in individual haem atoms involve the placement of haem propionate D. Within this group the largest displacement affects the CBD atom, which moves 1.1 Å towards the haem propionate A group. (CBD reflects the Brookhaven nomenclature for the haem structure that is widely used).

Structure of the His-64 → Thr MbN_3^- complex

N_3^- binds to the haem iron of the His-64 → Thr variant with a geometry similar to that observed for N_3^- bound to recombinant wild-type myoglobin (Figure 3 and Table 2). However, two conformations of the bound N_3^- are observed in the structure of the variant. The more prominent of these refined to 90% occupancy and thermal factors of 22, 28, and 28 Å² for the N-1, N-2 and N-3 atoms respectively. A comparison of the structure of this major orientation with that of the N_3^--free variant reveals that the distance from proximal ligand (His-93) to haem iron is 0.21 Å longer with the N_3^- bound (Table 2). This change seems to be a direct result of haem iron's movement into the porphyrin plane on binding of N_3^-. In addition, two new water molecules, Wat-157 and Wat-158 (Figure 3), are present in the distal haem pocket, and these form a link from the N_3^- ligand to solvent at the surface of myoglobin. Wat-157 is closer to the N_3^- group and has a refined occupancy of 64% (thermal factor 44 Å²), whereas Wat-158 is located further away and refines to full occupancy (thermal factor 30 Å²).

The N_3^- complexes of the variant also exhibit low-level electron density directed from the ligated N-1 nitrogen atom of bound N_3^- towards the protein surface in an omit difference electron density map. This density, together with the incomplete occupancies of this group and Wat-157, suggests the presence of a second minor conformation for bound N_3^-. This observation is in agreement with the results from the EPR measurements. The limited space available in the distal haem pocket would require exclusion of the low-occupancy water molecule, Wat-157, for N_3^- to bind in this orientation. Refinement of an N_3^- molecule at this alternative position was unsuccessful, probably as a result of the low occupancy of the N-2 and N-3 azide atoms in this orientation. This second N_3^- conformation was therefore modelled manually by fitting the observed electron density to produce the structure illustrated in Figure 3.

On the basis of a least-squares superposition of all main-chain atoms, the overall average value for main-chain atom positional differences between the structures of the His-64 → Thr variant

Figure 3 Stereo diagrams derived from crystallography determined structures of the haem and surrounding residues of wild-type and His-64 → Thr variant horse heart myoglobin in the presence and absence of N_3^-

(**a**) Aquo (thin lines) and azido (thick lines) wild-type horse heart metmyoglobin; (**b**) aquo (thin lines) and azido (thick lines) His-64 → Thr variant metmyoglobin; (**c**) minor N_3^- conformation observed in the His-64 → Thr variant; (**d**) orientation of N_3^- bound to wild-type (thin lines) horse heart myoglobin, the His-64 → Thr variant (medium lines), and the N_3^- complex of sperm whale myoglobin (thick lines) (PDB entry 2MBA).

Table 2 Haem co-ordination geometry in wild-type and His-64 → Thr metmyoglobins and their N_3^- derivatives

Structural element	Wild-type	His-64 → Thr	Wild-type MbN_3^-	His-64 → Thr MbN_3^-
Distance (Å)				
Fe–His-93 NE2	2.12	1.93	2.06	2.14
Fe–Wat-156 O	2.17	—	—	—
Fe–N_3^- N1	—	—	2.11	2.11
Fe–haem NA	2.03	2.04	2.01	2.03
Fe–haem NB	2.02	2.01	2.03	1.99
Fe–haem NC	2.00	2.99	2.00	2.01
Fe–haem ND	1.98	2.00	1.97	1.99
Fe out of plane*	0.09	0.28	0.07	0.10
Ser-92 OG1–His-93	3.18	3.21	3.30	2.76
Angle (degrees)				
Fe–ligand†	—	—	119.3	121.1

* Distance of the haem iron atom from the mean plane of the porphyrin ring. For this calculation the porphyrin ring is defined by the five atoms in each of the four pyrrole rings, the four bridging methine carbon atoms, the first carbon of each of the eight side chains of the haem and the central iron atom of the haem (33 atoms in total).

† Angle between the Fe–N_3^- co-ordination bond and the linear ligand direction.

with and without bound N_3^- is 0.28 Å (Figure 4). The two regions of greatest positional shift are at the N-terminus (residue 1, Δd 0.66 Å) and C-terminus (residues 152–153, Δd 0.80 Å) of the polypeptide chain. As can be seen in Figure 4, the positions of the haem group in these structures are comparable and exhibit an average positional shift of 0.24 Å for all 43 haem atoms on the basis of a fit of all main-chain atoms in the polypeptide chain. This value is decreased to 0.12 Å if haem atoms alone are used to obtain an overlap fit. Groups in the haem pocket that undergo substantial positional shifts between the N_3^--bound and N_3^--unbound forms of the variant include the side chains of Ser-92 and His-93, as well as the propionate D group of the haem. In particular, differences in side chain torsional angles are observed in χ_1 for Ser-92 ($\Delta = 22°$) and χ_2 for His-93 ($\Delta = 15°$). These changes result in a shortening of the Ser-92 OG to His-93 NE2 hydrogen bond by 0.45 Å. In contrast, these hydrogen bond distances are comparable in the N_3^--bound and N_3^--unbound forms of recombinant wild-type metmyoglobin (Figure 3).

Binding of N_3^- to either wild-type myoglobin or the His-64 → Thr variant results in increased thermal factors for part of the flexible CD connecting loop (residues 44–50) and part of the D helix (residues 51–58). In contrast, another region in the protein centred on position 80, part of the EF connecting loop, exhibits a marked decrease in thermal factors on N_3^- binding. These affected regions are all some distances from the haem and more than 15 Å from the site of N_3^- binding.

DISCUSSION

The present paper reports the first structure of the N_3^- complex of horse heart myoglobin and the first such structure of a myoglobin variant. As observed in the high-resolution structure of sperm whale azidometmyoglobin [18], N_3^- binds to horse heart myoglobin in a bent orientation. The Fe–N-1–N-3 angle is 119°, which compares with 117° observed for sperm whale myoglobin [18] and 111° reported for the Fourier difference analysis of the sperm whale MbN_3^- complex [17]. The N_3^- is oriented in the distal crevice near Ile-107 such that the His-64 NE2 is within hydrogen-bonding distance of the N-1 atom of the bound N_3^-. In aquometmyoglobin the co-ordinated water ligand is a hydrogen bond donor to His-64 NE2. In contrast, the co-ordinated N_3^- is a hydrogen bond acceptor. Contrary to expectation, accommodation of the N_3^- ligand in the distal pocket requires minimal rearrangement of active-site residues, with only the Leu-29 side chain and the haem group undergoing small displacements on N_3^- binding (Figure 1a). In contrast, distant backbone atoms of the CD corner, part of the D helix and the EF corner exhibit greater mobility. Greater backbone flexibility might result from accommodating the N_3^- ligand. However, a mechanism that explains this observation is not apparent at present.

A high-resolution structure has also been reported for the N_3^- complexes of *Aplysia limacina* myoglobin [39]. However, the active site of *Aplysia* myoglobin lacks the distal His-64 residue, and the bound azide is oriented towards the surface exposed portion of the distal site crevice to form a hydrogen bond with Arg-66 that is directed into the haem pocket in the presence of anionic ligands [40,41]. In contrast, we now know that N_3^- bound to two species of mammalian myoglobins is directed into the haem pocket [17,18].

The conformation of N_3^- binding can be regarded as an attempt to maximize the overlap of the haem iron atom d orbitals with the N_3^- nitrogen π orbital and to minimize van der Waals repulsion with the haem group atoms and those of adjacent side chains. The N_3^- binding configuration is the steric solution to maximizing the distance of the ligand from residues Phe-43, His-64 and Val-68. Interestingly, however, the binding angle and distances are similar to those observed in N_3^- bound to free haem [42]. As a result of the four-fold nature of the haem group, the N_3^- could bind to free haem with the N-3 atom directed to any of the four methine bridges. For the haem in wild-type myoglobin, three of these four positions are blocked by residues Phe-43, His-64 and Val-68. It is conceivable that the removal of any of these residues might permit N_3^- to bind in an alternative orientation. Indeed, our crystallographic and spectroscopic results indicate that two N_3^- orientations can occur in the His-64 → Thr variant (Figure 3c). The EPR spectrum of the His-64 → Thr variant exhibits two low-spin forms that are indicative of two different ligand conformations. In the major form, the N_3^- is oriented into the haem pocket (90% occupancy) and in the minor form the N_3^- is probably positioned towards the solvent (this configuration of the N_3^- could not be refined). Replacement of His-64 with threonine opens a channel that is occupied by two water molecules in the major conformation. In this case, replacement of His-64 and the charged nature of the N_3^- ligand increases the polarity of the distal pocket to favour

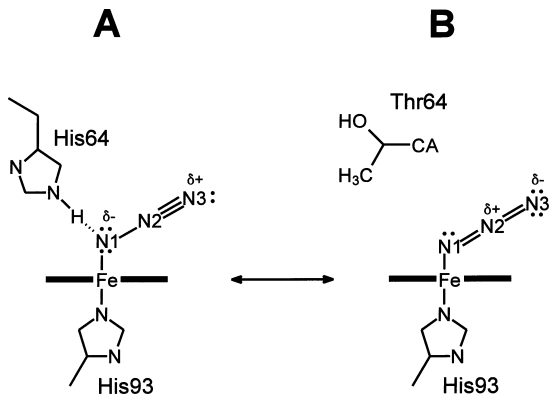

Scheme 1 Two canonical forms of N_3^- bound to the haem iron atom of metmyoglobin

the presence of two water molecules. In the minor orientation, N_3^- is within hydrogen-bonding distance of Wat-158 (Figure 1, trace C). One limiting factor in the occupancy of this minor N_3^- conformation is the steric overlap with the CG2 atom of residue 64, which probably decreases the population of this orientation greatly.

The major N_3^- conformation in the X-ray structure refined to an occupancy of 90 %, whereas different ratios of the two forms are observed in the EPR spectra. As the EPR measurements can be performed only at cryogenic temperature (10 K), it seems likely that the minor orientation is stabilized at low temperature. Temperature-dependent changes in axial ligation of haem proteins have been observed in the Val-68 → His variant of horse heart myoglobin [43] and in variants of cytochrome *c* peroxidase [44–46]. The low occupancy of the second N_3^- conformation found in the three-dimensional structure is consistent with the FTIR analysis at higher temperature (277 K). In this work the spectrum of the His-64 → Thr MbN_3^- complex could be fitted with just one low-spin band. If a greater amount of a second conformation had been present at 277 K, it should have been resolved in the FTIR spectrum.

Comparison of the three-dimensional structures of the N_3^- complexes of the His-64 → Thr and wild-type myoglobins reveals that the co-ordination geometry (see Table 2) and the orientation of the N_3^- ion in the distal pocket are similar in both proteins. Nevertheless, significant changes are observed in the FTIR spectra of the two N_3^- complexes. The ν_{max} of the asymmetric N_3^- stretch occurs at higher energy in the wild-type protein (2023.7, compared with 2018.6 cm^{-1} in His-64 → Thr). In work with inorganic N_3^- complexes, it has been found that the greater the difference between the two N–N distances, the higher the ν_{max} of the asymmetric N_3^- stretch [31]. Taking this observation into account, the differences in ν_{max} could be explained by the two resonance structures depicted in Scheme 1. In both the wild-type and the His-64 → Thr complexes a mixture of the two resonance structures (A and B) probably exists. However, in the wild-type protein the dominant form is likely to be that with the greater negative charge on the N-1 atom (Scheme 1A), which should result in stronger hydrogen-bonding interactions with the distal histidine residue. Predominance of this form would also result in relatively large differences in the two N–N distances and thus an increased stretching frequency. In the His-64 → Thr variant, no hydrogen-bonding interaction with the ligand exists, so form A is probably not as favoured as in the wild-type proteins; an equal population of both forms can therefore be assumed. A redistribution of resonance structures has been successfully used previously to explain changes observed in myoglobin variants studied by FTIR [38] and resonance Raman spectroscopy [13]. Another factor that could influence the ν_{max} is the increased polarity of the haem pocket in the His-64 → Thr variant. Enhanced polar interactions of N_3^- bound to the variant are apparent from the presence of two additional water molecules in the distal haem cavity. The electrostatic potential surrounding the bound ligand has been shown previously to be an important factor governing ν_{max} in CO and N_3^- binding to myoglobin [22,38].

In addition to the shift of ν_{max}, the N_3^- stretching bands of the variant are significantly broadened. The increased space in the haem cavity and the lack of the stabilizing hydrogen bond should permit greater conformational freedom for N_3^- bound to this variant. The thermal factors, which are an indication of atomic mobility, are similar for the N-1 atom in both the wild-type and variant proteins; however, the increased thermal factors observed for the N-2 and N-3 atoms in the variant indicate greater flexibility at the non-ligated end of the N_3^- group. We therefore attribute the broadening of the IR bands to a combination of several factors: increased mobility of the ligated N_3^-, increased solvent accessibility of the haem pocket, and the presence of a second low-occupancy N_3^- orientation.

We thank Nham Nguyen for skilful technical assistance. Atomic coordinates for the N_3^- complexes of the recombinant wild-type and His-64 → Thr horse heart myoglobins have been deposited with the Brookhaven Protein Data Bank. This work was supported by the Protein Engineering Network of Centres of Excellence. R.M. is the recipient of an MRC studentship; R.B. is the recipient of a postdoctoral fellowship from the Deutsche Forschungsgemeinschaft.

REFERENCES

1 Perutz, M. F. (1989) Trends Biochem. Sci. **14**, 42–44
2 Cutruzzola, F., Allocatelli, C. T., Ascenzi, P., Bolognesi, M., Sligar, S. G. and Brunori, M. (1991) FEBS Lett. **282**, 281–284
3 Adachi, S., Sunohara, N., Ishimori, K. and Morishima, I. (1992) J. Biol. Chem. **267**, 12614–12662
4 Allocatelli, C. T., Cutruzzola, F., Brancaccio, M., Brunori, M., Qin, J. and La Mar, G. N. (1993) Biochemistry **32**, 6041–6049
5 Huang, X. and Boxer, S. G. (1994) Nature Struct. Biol. **1**, 226–229
6 Theriault, Y., Pochapsky, T. C., Dalvit, C., Chiu, M. L., Sligar, S. G. and Wright, P. E. (1994) J. Biomol. NMR **4**, 491–504
7 Lambright, D. G., Balasumbramanin, S., Decatur, S. M. and Boxer, S. G. (1994) Biochemistry **33**, 5518–5525
8 Smerdon, S. J., Krzywda, S., Brzozowski, A. M., Davies, G. J., Wilkinson, A. J., Brancaccio, A., Cutruzzola, F., Allocatelli, C. T., Brunori, M., Li, T. et al. (1995) Biochemistry **34**, 8715–8725
9 Springer, B. A., Sligar, S. G., Olson, J. S. and Phillips, Jr., G. N. (1994) Chem. Rev. **94**, 699–714
10 Morikis, D., Champion, P. M., Springer, B. A. and Sligar, S. G. (1989) Biochemistry **28**, 4791–4800
11 Ikeda-Saito, M., Hori, H., Andersson, L. A., Prince, R. C., Pickering, I. J., George, G. N., Sanders, C. R. I., Lutz, R. S., McKelvey, E. J. and Mattera, R. (1992) J. Biol. Chem. **267**, 22843–22852
12 Biram, D., Garratt, C. J. and Hester, R. E. (1993) Biochim. Biophys. Acta **1163**, 67–74
13 Biram, D. and Hester, R. E. (1994) Biochim. Biophys. Acta **1204**, 207–216
14 Rohlfs, R. J., Mathews, A. J., Carver, T. E., Olson, J. S., Springer, B. A., Egeberg, K. D. and Sligar, S. G. (1990) J. Biol. Chem. **26**, 3168–3176
15 Quillin, M. L., Arduini, R. M., Olson, J. S. and Phillips, G. N. (1993) J. Mol. Biol. **234**, 140–155
16 Bogumil, R., Maurus, R., Hildebrand, D. P., Brayer, G. D. and Mauk, A. G. (1995) Biochemistry **31**, 10483–10490
17 Stryer, L., Kendrew, J. C. and Watson, H. C. (1964) J. Mol. Biol. **8**, 96–104
18 Rizzi, M., Ascenzi, P., Coda, A., Brunori, M. and Bolognesi, M. (1993) Remd. Fis. Acc. Lincei. **4**, 65–73
19 Perutz, M. F. and Mathews, F. S. (1966) J. Mol. Biol. **21**, 199–202
20 Deatherage, J. F., Obendorf, S. K. and Moffat, K. (1979) J. Mol. Biol. **134**, 419–429

21 Brancaccio, A., Cutruzolla, F., Allocatelli, C. T., Brunori, M., Smerdon, S. J., Wilkinson, A. J., Dou, Y., Keenan, D., Ikeda-Saito, M., Brantley, Jr., R. E. and Olson, J. S. (1994) J. Biol. Chem. **269**, 13843–13853
22 Bogumil, R., Hunter, C. L., Maurus, R., Tang, H.-L., Lee, H., Lloyd, E., Brayer, G. D., Smith, M. and Mauk, A. G. (1994) Biochemistry **33**, 7600–7608
23 Guillemette, J. G., Matsushima-Hibiya, Y., Atkinson, T. and Smith, M. (1991) Protein Eng. **4**, 585–592
24 Lloyd, E. and Mauk, A. G. (1994) FEBS Lett. **340**, 281–286
25 Evans, S. V. and Brayer, G. D. (1990) J. Mol. Biol. **213**, 855–897
26 Maurus, R., Overall, C. M., Bogumil, R., Luo, Y., Mauk, A. G., Smith, M. and Brayer, G. D. (1997) Biophys. Biochim. Acta., **1341**, 1–13
27 Higashi, T. (1990) J. Appl. Cryst. **23**, 253–257
28 Sato, M., Yamamoto, M., Imada, K., Katsube, Y., Tanake, N. and Higashi, T. (1992) J. Appl. Cryst. **25**, 348–357
29 Rossman, M. G., Leslie, A. G. W., Abdel-Meguid, S. S. and Tsukihara, T. (1979) J. Appl. Cryst. **12**, 570–581
30 Hendrikson, W. A. and Konnert, J. (1981) in Biomolecular Structure, Function, Configuration and Evolution, Vol. 1, (Srinivasan, R., ed.), pp. 43–57, Pergamon Press, Oxford
31 Dori, Z. and Ziola, R. F. (1973) Chem. Rev. **73**, 247–254
32 Luzzati, P. V. (1952) Acta Crystallogr. **5**, 803–810
33 Cruickshank, D. W. J. (1949) Acta Crystallogr. **2**, 65–82
34 Cruickshank, D. W. J. (1954) Acta Crystallogr. **7**, 519
35 Cruickshank, D. W. J. (1985) Fourier Synthesis and Structure Factors, 3rd edn., vol. 2, Reidel, Dordrecht
36 Sono, M. and Dawson, J. H. (1982) J. Biol. Chem. **257**, 5496–5502
37 Balasubramanian, S., Lambright, D. G. and Boxer, S. G. (1993) Proc. Natl. Acad. U.S.A. **90**, 4718–4722
38 Li, T., Quillin, M. L., Philips, Jr., G. N. and Olson, J. S. (1994) Biochemistry **33**, 1433–1446
39 Mattevi, A., Gatti, G., Coda, A., Rizzi, M., Ascendi, P., Brunori, M. and Bolognesi, M. (1991) J. Mol. Recogn. **4**, 1–6
40 Qin, J., La Mar, G., Ascoli, F., Bolognesi, M. and Brunori, M. (1992) J. Mol. Biol. **224**, 891–897
41 Conti, E., Moser, C., Rizzi, M., Mattevi, A., Lionetti, C., Coda, A., Ascenzi, P., Brunori, M. and Bolognesi, M. (1993) J. Mol. Biol. **233**, 498–508
42 Adams, K. M., Rasmussen, P. G., Scheidt, W. R. and Hatano, K. (1979) Inorg. Chem. **18**, 1892–1899
43 Lloyd, E., Hildebrand, D. P., Tu, K. M. and Mauk, A. G. (1995) J. Am. Chem. Soc. **117**, 6434–6438
44 Ferrer, J. C., Turano, P., Banci, L., Bertini, I., Morris, I. K., Smith, K. M., Smith, M. and Mauk, A. G. (1994) Biochemistry **33**, 7819–7829
45 Turano, P., Ferrer, J. C., Cheesman, M. R., Thomson, A. J., Banci, L., Bertini, I. and Mauk, A. G. (1995) Biochemistry **34**, 13896–13905
46 Bujons, J., Dikiy, A., Ferrer, J. C., Banci, L. and Mauk, A. G. (1996) Eur. J. Biochem. **243**, 72–84

Received 22 August 1997/14 January 1998; accepted 26 January 1998